Preprints (www.preprints.org) | NOT PEER-REVIEWED | Posted: 23 November 2021 doi:10.20944/preprints202111.0430.v1

Two compounds of 1-((4-bromothiophen-2-yl)methylene)-2-(perfluorophenyl)hydrazine, and 1-((4-bromo-5-methylthiophen-2-yl)methylene)-2-(perfluorophenyl)hydrazine and they crystal, molecular and electronic properties

Július Sivý[a], Dušan Bortňák[b], Daniel Végh[b] and Erik Rakovský[c]

[a]*Faculty of Mechanical Engineering, SUT, Námestie slobody 17, Bratislava 1, SVK-81231, The Slovak Republic*
[b]*Institute of Organic Chemistry, Catalysis and Petrochemistry, Faculty of Chemical and Food Technology, SUT, Radlinského 9, Bratislava 1, SVK-812 37, The Slovak Republic*
[c]*Department of Inorganic Chemistry, Faculty of Natural Sciences, Comenius University, Ilkovičova 6, Bratislava 4, SVK-842 15, The Slovak Republic*
E-mail: julius.sivy@stuba.sk

Abstract

The crystals, C11H4BrF5N2S, (**I**), 1-((4-bromothiophen-2-yl)methylene)-2-(perfluorophenyl)hydrazine and C12H6BrF5N2S, (**II**), 1-((4-bromo-5-methylthiophen-2-yl)methylene)-2-(perfluorophenyl)hydrazine are molecules with two rings and hydrazone part like a centre of the molecule. The compounds have been synthesized and characterized by elemental, spectroscopic (^{1}H-NMR) analysis. The crystal structures of the solid phase were determined by single crystal X-ray diffraction method. They crystallize in the monoclinic space group with $Z = 4$ and $Z = 2$ molecules per unit-cell. The compound (**I**) crystallizes as a racemate in the centrosymmetric space group and the compound (**II**) crystallizes as a non-racemate in the non-centrosymmetric space group. The "absolute configuration and conformation for bond values" were derived from the anomalous dispersion (ad) for (**II**). The crystal structures are revealed diverse non-covalent interactions such as intra- and interhydrogen bonding, π-ring···π-ring, C-H···π-ring and they were investigated. The expected stereochemistry of hydrazones atoms C7, N2 and N1 were confirmed for (**I**) and (**II**). The hole molecule of the (**I**), and (**II**) possesses "a boat conformation" like a 6-membered ring. The results of the single crystal studies are reproduced with the help of Hirshfeld surface study and Gaussian software.

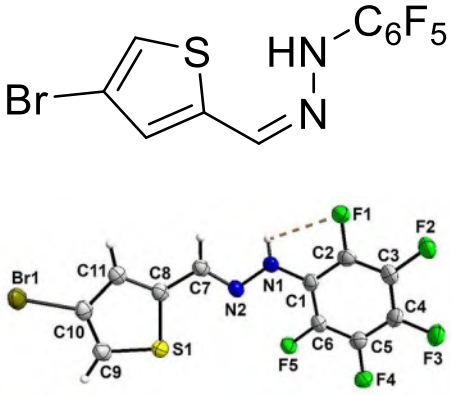

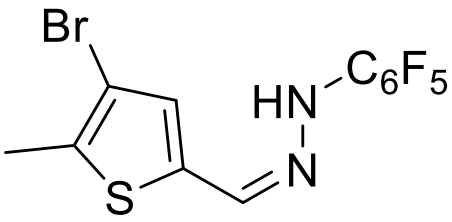

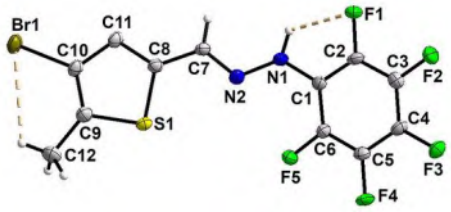

Keywords: *Ab initio* DFT/B3LYP/6-311G/Auto calculation, hydrazine, Hirshfeld surface, hydrogen interactions, single-crystal X-ray study

Introduction

Microbial resistance to antibiotics is an urgent and worldwide well-known. Several hydrazones were synthesized by using benign reaction conditions. These molecules are potent growth inhibitors of drug-resistant strains of Staphylococcus aureus and Acinetobacter baumannii with minimum inhibitory concentration values. Molecules are nontoxic to human cells at appropriate concentrations. Although hydrazones possess greater intrinsic hydrolytic stability than the corresponding imines but still these molecules can be converted into the starting mate-rials by reacting with water under the physiological condition. The antimicrobial activity of the compounds, hydrazones, may due to the hydrolyzed products, aldehydes, and hydrazines. For example, the aldehyde derivative did not show any activity, but the hydrazine showed weak growth inhibition. Thus, we can conclude that the antimicrobial activity of the compounds is due to their hydrazone functional groups not due to their possible hydrolyzed products. Fluorine substitution has been extensively studied in drug discovery to enhance the biological activity and increase the chemical and metabolic stability of the resultant molecules. We designed and synthesized hydrazone derivatives not only for antimicrobial studies. Hydrazones are of general wide interest not only in medicinal chemistry[1-6] but also in material chemistry,[7-16] the compounds exhibit nematicidal and insecticidal activity.[17] N-pentafluorophenyl substituted hydrazones can also be used as analytical reagents. Two principles are most often used in the analysis:

1. Interaction of an ion (anion, cation) with a secondary amino group while observing a color change after the addition of the analyte.
2. Formation of a stable molecular ion or a fragment that is well detectable in mass spectrometry. (usually pentafluorophenyl).

On the 1st principle, ions such as the copper cation as well as the fluoride anion[18,19] (Scheme 1, 2, 3) can be well determined, and it is generally difficult to determine and currently its detection is a "hot problem". Fluorine is the thirteenth most abundant element on earth and occurs mainly in the form of the minerals fluorite, fluorapatite and cryolite. In the form of organic compounds, only twelve individual compounds have been

identified in nature, virtually all of which show considerable toxicity. Despite the low occurrence of fluoroorganic compounds in nature, which are without exception highly toxic, chemical research and industry are currently producing thousands of new fluorine-containing organic compounds. The year 1941 is considered to be the beginning of synthetic fluoroorganic chemistry. According to data from the Internet, global demand for fluorine-containing chemicals in 2015 reached 3.35 million tons per year. Due to the wide range of issues in different works, the crystal, molecular and electronic properties of *N*-pentafluorophenyl hydrazones will be discussed. These compounds showed diverse crystal-molecular interactions which includes interactions such as π···π, C-H···π and so on. We analyse the crystal-base structural properties by single crystal X-ray diffraction method, Gaussian method and by the Hirshfeld surface. We report the synthesis here, molecular, crystal and electronic structure of the title compounds, (**I**) and (**II**).

The interest of our research group is in the developing of novel hydrazone derivatives routes for they synthesis in simple and efficient ways. The molecules of the title compounds crystallizes in the space group $P2_1/n$ and *Pn*. Accordingly, the compound (**I**) is a racemate and consists of one molecule in the independent part of the unit-cell with relative configuration of carbon atoms and the compound (**II**) is a non-racemate and consists of one molecule in the independent part of the unit-cell. Hydrazone part of the molecule and left and right side of the molecule possesses "a boat conformation" like a 6-membered ring. The first right-side ring, hexafluorophenyl, is planar and adopts a plane conformation, while atom N1 is displaced from these plane with the out-of-plane displacement of 0.011 (3) for (**I**) and 0.032 (7) Å for (**II**), than out-of-plane displacement for atoms F1, F2, F3, F4, F5 is 0.078 (3), -0.039 (3), -0.014 (3), 0.018 (3), -0.027 (3) for (**I**) and 0.074 (7), -0.030 (8), 0.011 (7), -0.008 (7), -0.047 (6) Å, (**II**). The second left-side ring, thiophene, is planar too, the out-of-plane displacement for the atom Br1 is -0.012 (3) for (**I**) and -0.008 (7), (**II**) and for the atom C12 is 0.061 (9) Å, (**II**). The dihedral angle for (**I**) between the planes is 31.99 (5)° and 31.77 (11)° for (**II**). The compounds (**I**) and (**II**) were investigated by *ab initio* DFT/B3LYP/6-311G/Auto and calculation were performed. The properties of the conformation of the products (**I**) and (**II**) were controlled by X-ray structure determination. Crystal structure of the title compound (**I**) (Scheme 1) as a hydrazone derivative crystallizes in the centrosymmetric space group, and crystal structure of the compound (**II**) (Scheme 2) as the hydrazone derivative crystallizes in the non-centrosymmetric space group (monoclinic crystal system). Simple Hirshfeld surface analysis was used to visualize the map for the different intermolecular interactions in the crystal structure and Gaussian natural bond order analysis was performed.[20]

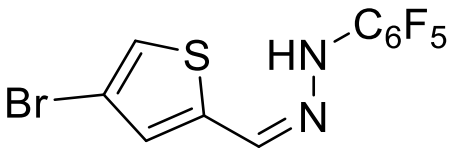

Scheme 1 View of the molecular structure of the title compound (**I**).

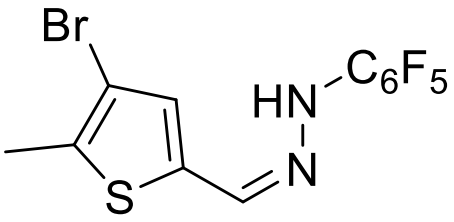

Scheme 2 View of the molecular structure of the title compound (**II**).

Results and Discussion

The start "configuration" of the molecules in absolute formulation is known from the synthesis and "stereochemistry" of atoms in the molecules was confirmed. Molecular geometry and atom numbering scheme of the (**I**) and (**II**) are shown in Figs. 1, 3. Molecular crystal packing view of the (**I**) and (**II**) are shown in Figs. 2, 4 and experimental details of the compounds (**I**) and (**II**) are listed in Table 1, selected geometric parameters are listed in Tables 3 and 5.

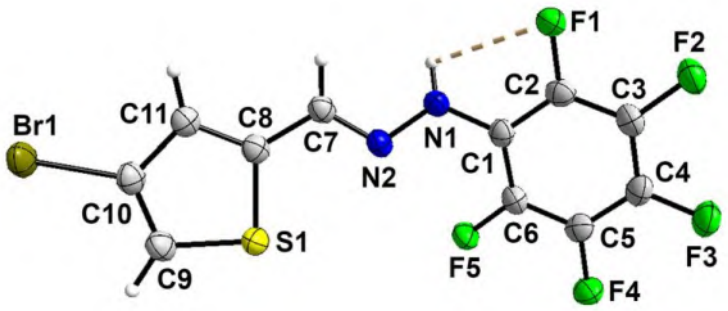

Figure 1 The molecular structure of the title compound (**I**) with the atomic numbering scheme. Displacement ellipsoids are drawn at the 50% probability level.

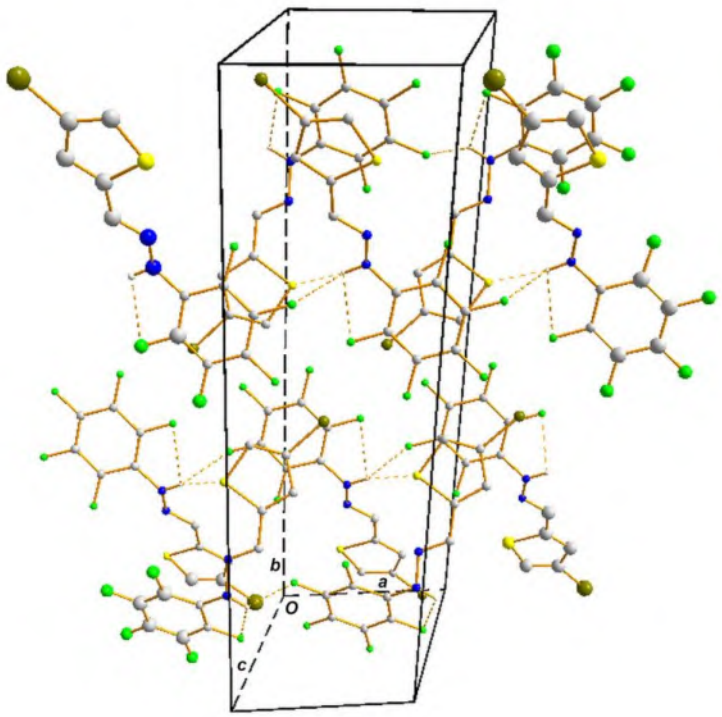

Figure 2 Part of the crystal structure of the title compound (**I**) showing the formation of intra- and intermolecular hydrogen interactions. The chains of molecular structure of the title compound extending along the *a* axis. H atoms not involved in the motif have been omitted.

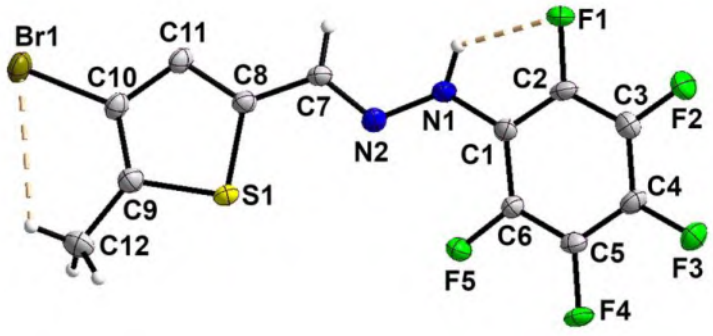

Figure 3 The molecular structure of the title compound (**II**) with the atomic numbering scheme. Displacement ellipsoids are drawn at the 50% probability level.

Preprints (www.preprints.org) | NOT PEER-REVIEWED | Posted: 23 November 2021 doi:10.20944/preprints202111.0430.v1

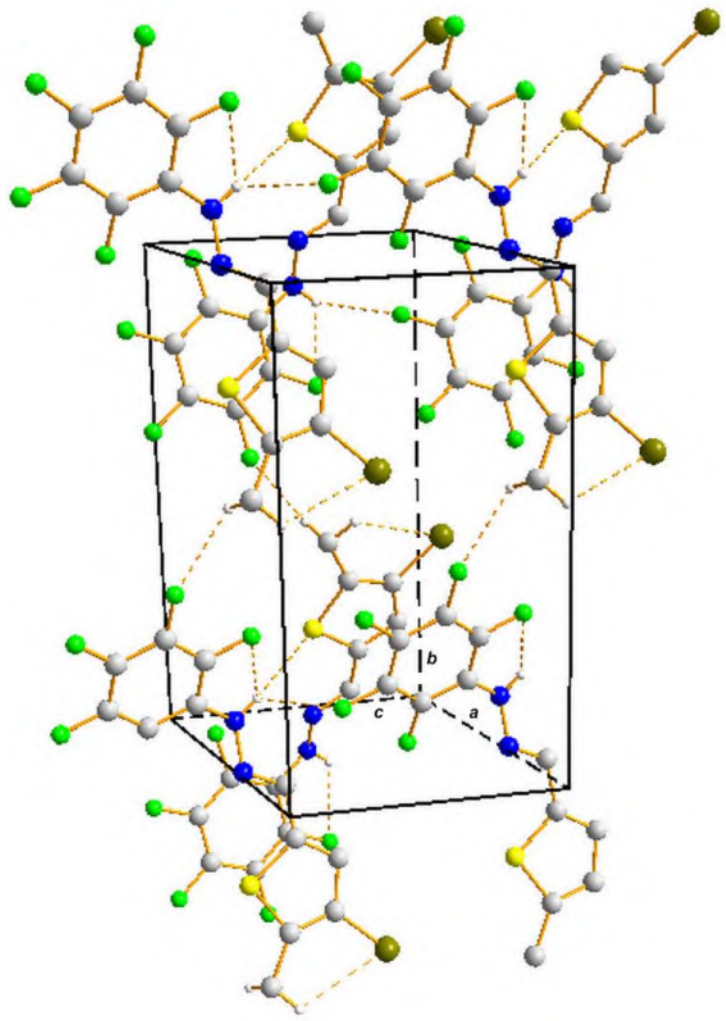

Figure 4 Part of the crystal structure of the title compound (**II**) showing the formation of intra- and intermolecular hydrogen interactions. The chains of molecular structure of the title compound extending along the *c* axis. H atoms not involved in the motif have been omitted.

Preprints (www.preprints.org) | NOT PEER-REVIEWED | Posted: 23 November 2021 doi:10.20944/preprints202111.0430.v1

Table 1 Experimental details of the compounds (**I**)[a] and (**II**)[b].

Empirical formula	$C_{11}H_4BrF_5N_2S$	$C_{12}H_6BrF_5N_2S$
Formula weight	371.13	385.16
Temperature (K)	298(2)	298(2)
Wavelength (Å)	1.54178	0.71073
Crystal system	Monoclinic	Monoclinic
Space group	$P2_1/n$ (centro)	Pn (non-centro)
Unit-cell dimensions (Å, °)	a = 7.11250(10) b = 25.0194(5) c = 7.1935(2) β = 109.457(2)	a = 7.1916(3) b = 13.5415(5) c = 7.2384(4) β = 109.951(6)
Volume (Å^3)	1206.98(5)	662.61(6)
Z	4	2
Density (calculated) (Mg/m^3)	2.042	1.930
Absorption coefficient (mm^{-1})	6.826	3.311
F(000)	720	376
Crystal size (mm)	0.594 x 0.220 x 0.091	0.591 x 0.306 x 0.065
Theta range for data collection (°)	3.533 to 71.747	1.504 to 32.774
Index ranges	-8<=h<=8, -30<=k<=29, -8<=l<=8	-10<=h<=10, -20<=k<=20, -10<=l<=10
Reflections collected	32397	11109
Independent reflections	2331 [$R_{(int)}$ = 0.0402]	4379 [$R_{(int)}$ = 0.0508]
Completeness to theta (°, %)	67.679, 100.0	25.242, 100.0
Refinement method	Full-matrix least-squares on F^2	Full-matrix least-squares on F^2
Data/restraints/parameters	2331/0/184	4379/2/194
Goodness-of-fit on F^2	1.036	1.032
Final R indices [I>2⍰(I)]	R_1 = 0.0296, wR_2 = 0.0866	R_1 = 0.0447, wR_2 = 0.1013
R indices (all data)	R_1 = 0.0298, wR_2 = 0.0869	R_1 = 0.0531, wR_2 = 0.1097
Absolute structure parameter	-	0.007(7) (Flack)
Chemical absolute configuration	-	rmad
Extinction coefficient	-	-
Largest diff. peak and hole (e·Å^3)	0.523 and -0.832	1.063 and -1.137

[a]CCDC_2027085, [b]CCDC_2027086. Crystallographic data for the structures reported in this paper will be available from the Cambridge Crystallographic Data Centre.

Table 2 H-bond geometry and X-Y···π-centroid (Cg(1)) stacking interactions (Å, ^{o}) for (**I**).

D—H···A	D—H	H···A	D···A X-Y···Cg(1)	D—H···A
N1—H1···F1	0.87(3)	2.38(3)	2.739(2)	105(2)
N1—H1···F4^{i}	0.87(3)	2.55(3)	3.087(3)	121(2)
N1—H1···S1^{ii}	0.87(3)	2.74(3)	3.538(2)	152(2)
C3—F2···Cg(1)^{iii}			3.766(2)	

Symmetry codes: (^{i}) 1/2+x,1/2-y,1/2+z; (^{ii}) 1+x,y,z; (^{iii}) -1/2+x,1/2-y,-1/2+z; Cg(1): S1, C9, C10, C11, C8

Table 3 Selected geometric parameters for (**I**): bond lengths (Å), bond and torsion angles (^{o}).

C1-N1	1.393(3)	C7-N2-N1	115.73(17)
C7-N2	1.277(3)	N1-C1-C6-F5	0.8(3)
C8-S1	1.732(2)	N1-C1-C6-C5	-179.68(19)
C9-S1	1.717(2)	N2-C7-C8-C11	174.6(2)
C10-Br1	1.886(2)	N2-C7-C8-S1	-7.3(3)
N1-N2	1.383(2)	S1-C9-C10-C11	-0.2(2)
C7-C8	1.452(3)	S1-C9-C10-Br1	179.47(11)
C2-C1-N1	120.40(18)	Br1-C10-C11-C8	-179.73(15)
N1-C1-C6	123.03(19)	C2-C1-N1-N2	-138.44(19)
N2-C7-C8	119.23(18)	C6-C1-N1-N2	43.9(3)
N2-C7-H7	120.4	C8-C7-N2-N1	176.83(17)
C11-C8-S1	111.53(16)	C1-N1-N2-C7	162.23(18)
C7-C8-S1	120.84(15)	C10-C9-S1-C8	0.33(17)
C10-C9-S1	110.80(16)	C11-C8-S1-C9	-0.34(17)
C9-C10-Br1	123.26(16)	C7-C8-S1-C9	-178.76(17)
C11-C10-Br1	122.38(15)	N1-C1-C2-F1	2.1(3)
N2-N1-C1	117.00(17)	N1-C1-C2-C3	-178.16(18)
C9-S1-C8	91.86(10)		

Table 4 H-bond geometry and X-Y···π-centroid (Cg(1)) stacking interactions (Å, °) for (**II**).

D—H···A	D—H	H···A	D···A X-Y···Cg(1)	D—H···A
C12—H12C···Br1	0.96	2.90	3.365(6)	110(7)
N1—H1···F1	0.83(7)	2.29(6)	2.748(5)	115(6)
C12—H12B···F2^{i}	0.96	2.53	3.135(6)	121(3)
N1—H1···S1^{iii}	0.83(7)	2.89(7)	3.620(5)	148(6)
N1—H1···F4^{ii}	0.83(7)	2.56(7)	3.084(6)	122(6)
C3—F2···Cg(1)^{iv}			3.757(4)	
C6—F5···Cg(1)^{v}			3.925(4)	

Symmetry codes: (^{i}) x,y+1,z; (^{ii}) x,y,z-1; (^{iii}) x-1/2,-y,z-1/2; (^{iv}) 1/2+x,-y,1/2+z; (^{v}) -1/2+x,-y,1/2+z; Cg(1): S1, C9, C10, C11, C8.

Table 5 Selected geometric parameters for (**II**): bond lengths (Å), bond and torsion angles (°).

C1-N1	1.391(6)	C7-N2-N1	116.6(4)
C7-N2	1.279(6)	C8-S1-C9	92.7(2)
C7-C8	1.448(7)	N1-C1-C2-C3	-177.9(5)
C9-S1	1.740(5)	N1-C1-C6-C5	179.8(5)
C10-Br1	1.883(5)	N2-C7-C8-C11	173.5(5)
N1-N2	1.379(6)	N2-C7-C8-S1	-8.1(6)
C2-C1-N1	119.8(4)	C12-C9-C10-Br1	2.7(8)
C6-C1-N1	123.4(4)	S1-C9-C10-Br1	-179.7(3)
N2-C7-C8	119.7(4)	Br1-C10-C11-C8	179.9(3)
C11-C8-S1	111.3(4)	C2-C1-N1-N2	-138.0(5)
C7-C8-S1	121.5(4)	C6-C1-N1-N2	44.2(7)
C10-C9-S1	109.2(4)	C8-C7-N2-N1	177.1(4)
C9-C10-Br1	122.2(4)	C1-N1-N2-C7	162.2(4)
C11-C10-Br1	122.8(4)	N2-N1-C1	117.7(4)

Central hydrazone part of the molecule is planar for the both compounds. Atom N1 possesses more negative net charge than N2 (Figs. 5, 6, NBO analysis). The molecular structures is moreover stabilized by one intramolecular N1—H1···F1 hydrogen bond(s) and one intramolecular C12—H12C···Br1 hydrogen interaction only for (**II**) with an H-atom as the donor, Figs. 1, 3, Tabs. 4, 5. The N2—N3 [1.379 (5)–1.383 (2) Å] distances are slightly shorter compared to the hydrazine Nsp^2—Nsp^2 (about 1.40 Å) single bond[36] and about 1.46 Å single bond[37], which indicate that there is a significant delocalization of π-electron density over the hydrazone portion of the molecule. The conformation of the N1—H1 group of the hydrazone part is advantageous for intramolecular H bond to the hexafluorophenyl part of the molecule(s). The unit-cell density for the parent compound (**I**) is 2.042 g/cm^3 (V = 1206.98, F(000) = 720.0, Mu = 6.83 mm^{-1}, Cell Wt = 1484.53, Rho = 2.042)[listing of 26]. The introduction of methyl-substituent to H atom of thiophene ring for (**II**) changed this to value of 1.930

Preprints (www.preprints.org) | NOT PEER-REVIEWED | Posted: 23 November 2021 doi:10.20944/preprints202111.0430.v1

g/cm^3 (V = 662.61, F(000) = 376.0, Mu = 3.31 mm^{-1}, Cell Wt = 770.32, Rho = 1.930)[listing of 26], respectively. The different values of the unit-cell densities indicate the role of the crystallizing process of the substituent on this parameter. The methyl-substituted compound has the lowest value for the unit-cell density.[listing of 26] The observed bond lengths and Wiberg bond indices of the compounds showed a clear distinction between single and double bonds in the central spacer unit and the rest of the molecules.[38] The atoms C7—C8 [1.452 (3), I_w = 1.110 and 1.448 (6), I_w = 1.118, Å] and N2=C7 [1.279 (6), I_w = 1.737 and 1.277 (3), I_w = 1.729, Å] interatomic distances confirm that they are single and double bonds, (Br1—C10: I_w = 1.033 and I_w = 1.027). Atom S1 representing strong stability effect for this molecule side part (net NBO charge 0.433 and 0.425, Figs. 5, 6).

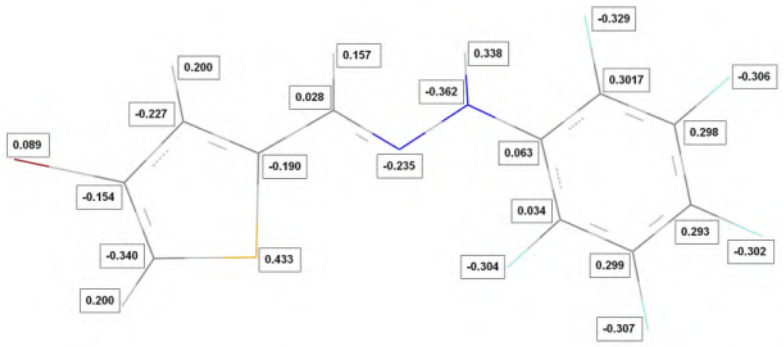

Figure 5 The molecular structure of the title compond (**I**) shoving the scheme for the net atomic charges (single point geometry, NBO analysis).

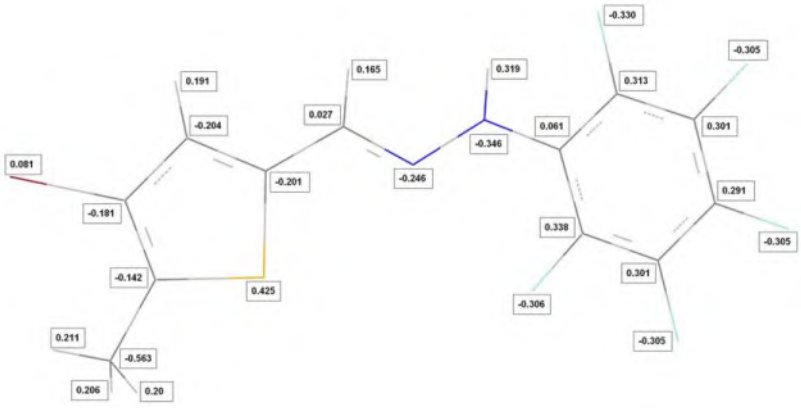

Figure 6 The molecular structure of the title compond (**II**) shoving the scheme for the net atomic charges (single point geometry, NBO analysis).

The torsion angle of C2, C1, N1, N2 atoms plays and suggests the fact that H1 atom participates in intra- and intermolecular hydrogen bonds. Figure 7 shows the best least-squares fit (RMS Error = 5.714 x 10^{-3} Å, atoms C1, N1, N2, C7, C8,) between two close molecules (**I**) and (**II**).[40] In the basic view we see how molecules fit together to form the importance of molecular structure in crystal structure.

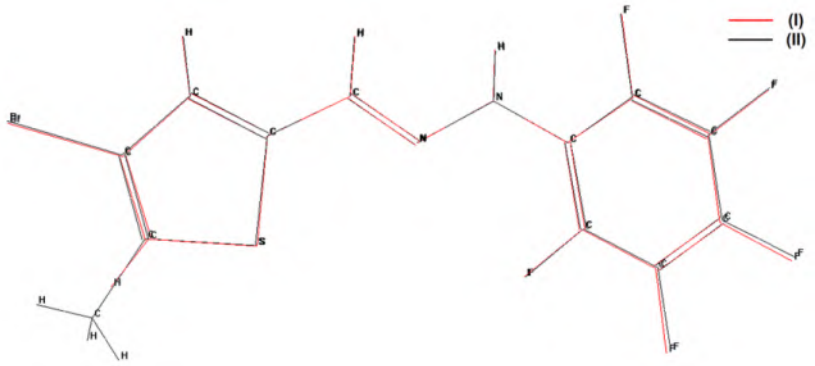

Figure 7 The molecular structure fit of the compounds (**I**) and (**II**) (RMS Error = 5.714 x 10^{-3} Å)[40].

Graph-set motif of the molecules was observed, it is a C(6),[39] Figs. 8, 9. Cremer-Pople puckering parameters

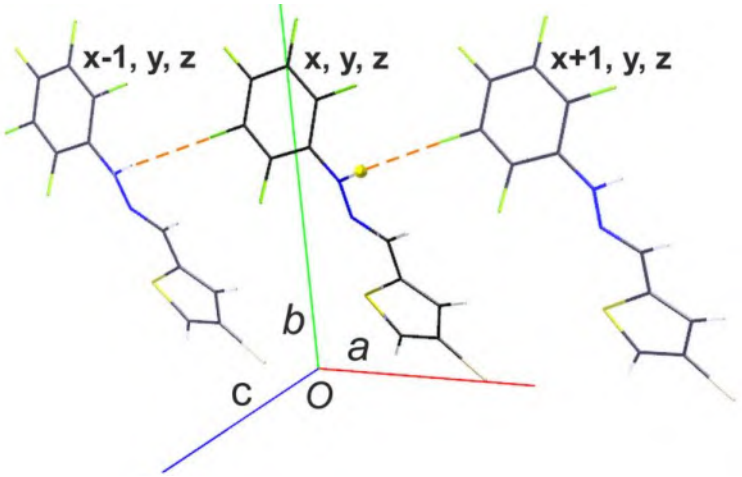

Figure 8 Molecular packing view of the crystal structure (**I**) shows the formation of the C(6) graph-set motif.

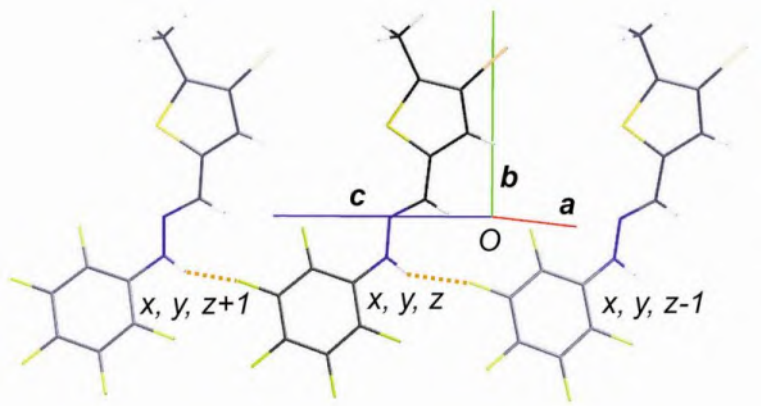

Figure 9 Molecular packing view of the crystal structure (**II**) shows the formation of the C(6) graph-set motif.

were not confirmed for both crystal structures. Molecular packing view of the crystal structures shows the formation of the X—Y···Cg(1) bond motifs, Figs. 10, 11.

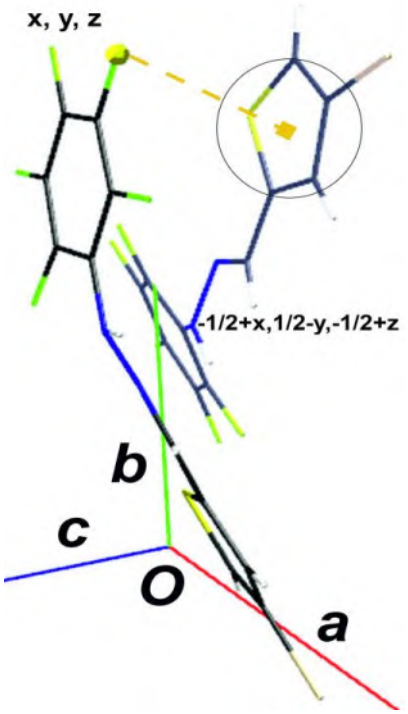

Figure 10 Molecular packing view of the crystal structure (**I**) shows the formation of the X—Y···Cg(1) bond motif.

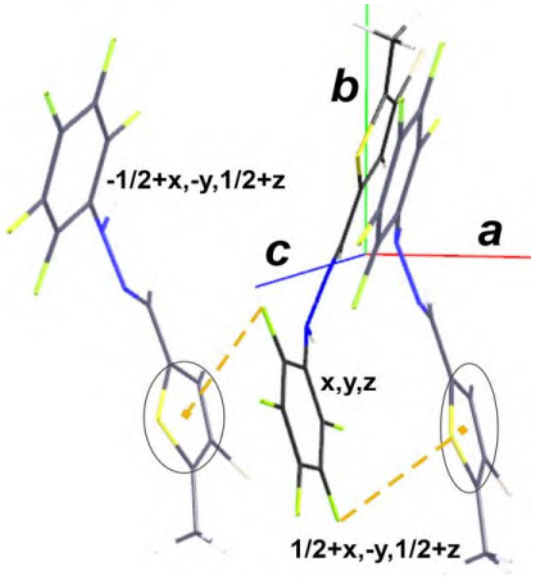

Figure 11 Molecular packing view of the crystal structure (**II**) shows the formation of the X—Y···Cg(1) bond motifs.

The results of these calculations are in a good agreement with the experimental values of bond lengths found by X-ray structure analysis. NBO analysis of theoretical calculations in vacuum (not adding any polarization functions) at the ab initio DFT/B3LYP level using the 6-311G/Auto basis set model (single point geometry = the crystal geometry was used, NBO net charges)[20] is shown for selected atoms in Figs. 5, 6. Hirshfeld surface analysis is a powerful tool for gaining additional view into the intermolecular interaction of molecular crystals. The size, shape and type of Hirshfeld surface allows the qualitative and quantitative investigation and visualization of intermolecular close contacts in molecular crystals. The structure and its Hirshfeld's approach is

Preprints (www.preprints.org) | NOT PEER-REVIEWED | Posted: 23 November 2021 doi:10.20944/preprints202111.0430.v1

for each molecule enclosed surface (Hirshfeld surface) such that in any point within it, that half or more of electron density comes from the atoms of molecule. The Hirshfeld surface map over d_{norm} analyse the electron density, the shape-index and the curvedness. Hirshfeld surface (Figs. 12, 13) shows a simple workable places for the biological activity with respect to the shortest distances of worthy molecule-hydrogen bonding to suitable receptors site-locality and from this point of view and the molecular "dimension", the biological activities will be as few as adequate (d_{norm} range (-0.187, 1.020) and d_{norm} range (-0.103, 1.118), the atoms within radius 3.80 Å). Hirshfeld surface analysis was carried out in order to study the nature of the hole surface molecular bond contacts of the title compounds. Hirshfeld surfaces were generated using CrystalExplorer 17.5 in order to analyse the nature of the intermolecular contacts and their quantitative contributions to the crystal packing in (**I**) and (**II**). The electrostatic potentials, obtained using TONTO integrated within CrystalExplorer using the DFT/B3LYP/6-31G basis set model[21-23], were involved to mapped Hirshfeld surfaces because of they were mapped over the electrostatic potentials.

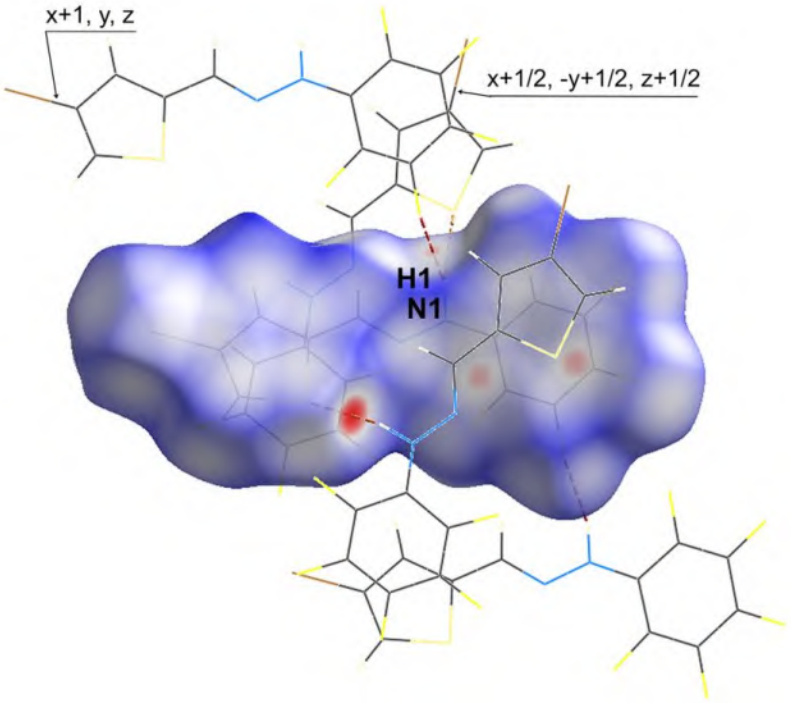

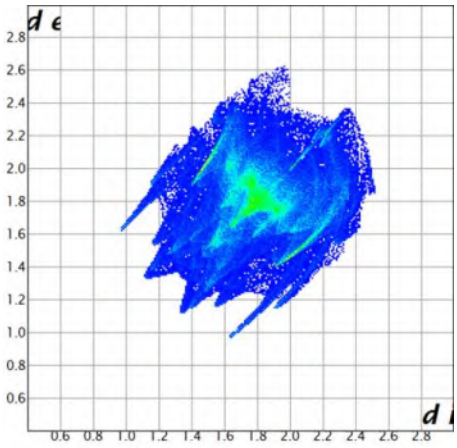

Figure 12 Simple Hirshfeld surface for the title compound (**I**), d_{norm} range (-0.187, 1.020), the atoms within radius 3.80 Å and corresponding (total) FingerPrint.

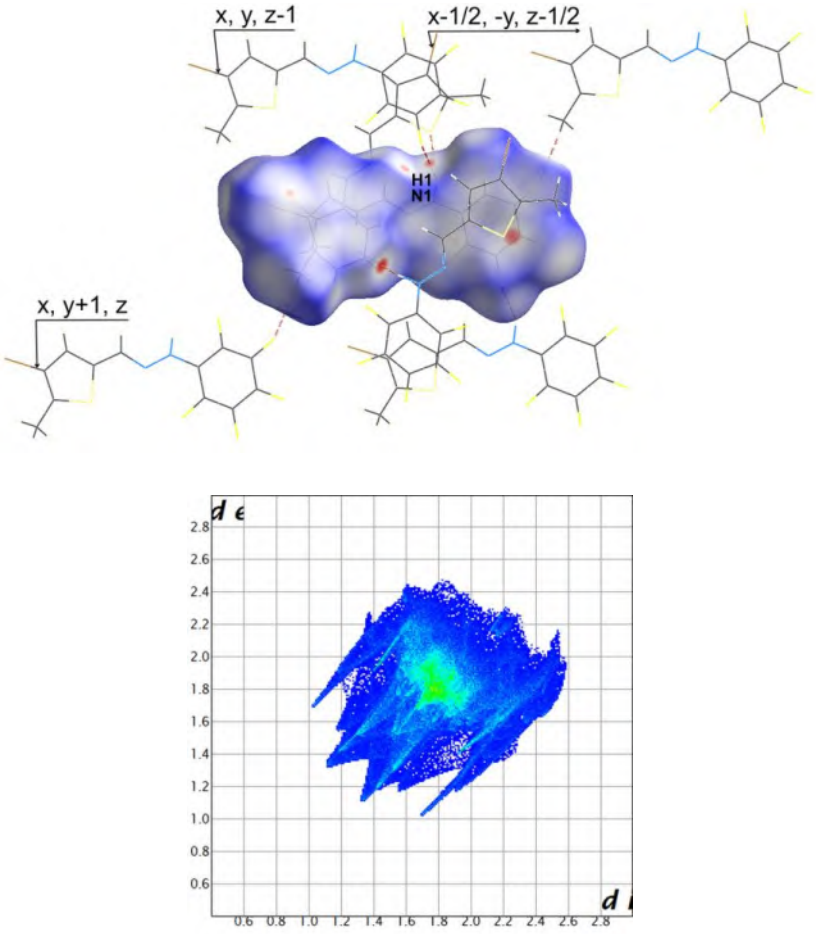

Figure 13 Simple Hirshfeld surface for the title compound (**II**) , d_{norm} range (-0.103, 1.118), the atoms within radius 3.80 Å and corresponding (total) FingerPrint.

Conclusions

To conclude, we synthesized 1-((4-bromothiophen-2-yl)methylene)-2-(perfluorophenyl)hydrazine and 1-((4-bromo-5-methylthiophen-2-yl)methylene)-2-(perfluorophenyl)hydrazine. We successfully carried out all NMR spectra, X-ray investigation and Gaussian analyses. Two hydrazone derivatives and its “chemical, molecular-structural, NBO charges, Hirshfeld surface and fitting interaction properties” were asserted from the experimental and theoretical work. The atoms of sulphur, nitrogen and “they” hydrogen(s) atom(s) play considerable role for the bond system in the hole molecule(s) and these atoms responsible participate in the crystal structure "configuration diversity" of the spatial forms of the molecules in the crystals. "Conformation diversity" was not observed in fitting scheme.

Preprints (www.preprints.org) | NOT PEER-REVIEWED | Posted: 23 November 2021 doi:10.20944/preprints202111.0430.v1

Experimental Section

Synthesis and crystallization.

The compounds (**I**) and (**II**) were prepared according to a standard protocol (Scheme 3) described in literature. All NMR spectra were obtained using an INOVA NMR 300 MHz spectrometer (operating frequencies 300 MHz (^{1}H), 75 MHz (^{13}C) and 282 MHz (^{19}F)) equipped by an inverse triple resonance probe and a standard tuneable X/H probe with the possibility to tune the high frequency channel to the resonance frequency of ^{19}F. Tetramethylsilane was used for the calculation of the ^{1}H and ^{13}C chemical shift scales and correctly referenced using the (residual) solvent signals (2.50 and 39.52 ppm for DMSO and 7.26 and 77.00 ppm for chloroform). $CFCl_3$ was used for the calculation of the ^{19}F chemical shift scale; in order to correctly reference the ^{19}F chemical shift scale an automatic referencing mechanism exploiting the ^{2}H signal of the deuterated solvent was used.

General procedure for synthesis of hydrazone.

To the solution of the corresponding aldehyde in 20 ml of ethanol is added ethanolic solution (10 ml) of the pentafluorophenylhydrazine. To this mixture a catalytic amount of concentrated hydrochloric acid were added (approximately 3-5 drops). The reaction mixture has been refluxed for 8 hours (under TLC + UV control). The solvent was evaporated under reduced pressure and the residue has been crystallized from ethanol to obtain the pentafluorophenylhydrazone (**I**) - (**II**).

1-((4-bromothiophen-2-yl)methylene)-2-(perfluorophenyl)hydrazine, (**I**), (Scheme 3)

4-bromothiophene-2-carbaldehyde (1.000 g, 5.23 mmol, 1 eq.) and pentafluorophenylhydrazine (1.037 g, 5.23 mmol, 1 eq.) were left to react in ethanol following the general procedure for the synthesis of hydrazones. The hydrazone (**I**) was obtained as a brown crystalline matter in a 51 % yield (0.991 g), m.p. 138-140 ^{o}C. ^{1}H NMR (300 MHz): δH=7.07 (d, J=1.3Hz , ^{1}H), 7.20 (d , J=1.1 Hz, ^{1}H), 7.88 (s, ^{1}H). 13C NMR (75 MHz): δC=109.88, 119.75, 124.26, 129.87 135.78, 136.05, 138.15, 139.67. ^{19}F NMR (282 MHz): δF= -165.80 (tt, J=3.8 Hz, J=21.6, 1F), -163.30 (dt, J=4.8 Hz, J=21.4, 2F), -155.64 (d, J=21.6, 2F).

1-((4-bromo-5-methylthiophen-2-yl)methylene)-2-(perfluorophenyl)hydrazine, (**II**) (Scheme 3)

4-bromo-5-methylthiophene-2-carbaldehyde (1.000 g, 4.88 mmol, 1 eq.) and pentafluorophenylhydrazine (0.966 g, 4.88 mmol, 1 eq.) were left to react in ethanol following the general procedure for the synthesis of hydrazones. The hydrazone (**II**) was obtained as a brown crystalline matter in a 60 % yield (1.127 g), m.p. 153-155 ^{o}C. ^{1}H NMR (300 MHz) δ 10.37 (s, ^{1}H), 8.17 (s, ^{1}H), 7.23 (s, ^{1}H), 2.34 (s, 3H). ^{13}C NMR (75 MHz) δ 137.7 (dm J=245 Hz), 137.3 (dm J=246 Hz) 137.2, 136.0, 135.0, 133,9 (dm J= 247Hz) 129.9, 120.8 (m) 108.7, 14.6. ^{19}F NMR (282 MHz): δF= -169.73 (m, 1F), -164.33 (m, 2F), -155.75 (m, 2F).[42]

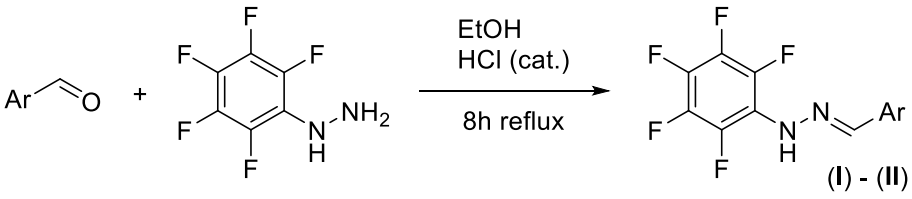

Ar= 4-bromothiophene-2-yl (**I**)
4-bromo-5-methylthiophene-2-yl (**II**)

Scheme 3

Refinement.

Manuals of "The CIF file, refinement details and validation of the structure, IUCr, 2011" and "User guide to crystal structure refinement with SHELXL, IUCr, 2008" pointed out the refinement rules for all H atoms, e.g., they were positioned with idealized geometry using a constrained riding model with C—H distances in the range of 0.93—0.98 Å (AFIX card was used) and non-idealized geometry N—H distance in the range of 0.83—0.87 Å (AFIX card was omitted)[26]. The U_{iso}(H) values were set to 1.2U_{eq} (*C*-aromatic, N) and 1.5U_{eq} (C-methyl), respectively.

Data collection.

Crystal data and conditions of data collection and refinement are reported in Table 1. Data collection: Pilatus300K StoeStadivari,[32-35,41] program(s) used to solve structure,[24-25] program(s) used to refine structure,[26] molecular graphics,[27] software used to prepare material for publication.[20-23,26,28,29,30,31]

Acknowledgements

This work was supported by the Slovak Research and Development Agency under the contract no. APVV-17-0513 and by the Scientific Grant Agency of the Slovak Republic KEGA (Project No. 027STU-4/2019). This contribution is also the result of the project: Research Center for Industrial Synthesis of Drugs, ITMS 26240220061, supported by the Research & Development Operational Program funded by the ERDF. We are grateful to the HPC center at the Slovak University of Technology in Bratislava, which is a part of the Slovak Infrastructure of High Performance Computing (SIVVP project, ITMS code 26230120002, funded by the European region development funds, ERDF), for the computational time and resources made available.

References

1. Verma, G.; Marella, A.; Shaquiquzzaman, M.; Akhtar, M.; Ali, M. R.; Alam, M. M. *J. of Pharmacy and Bioallied Sciences.* **2014**, Medknow Publications, 69, https://doi.org/10.4103/0975-7406.129170.
2. Kuman, L.; Chauhan L. *J. Chem. Pharm. Res.* **2014**, 6 (12), 916.
3. Giliberti, G.; Ibba, C.; Marongiu, E.; Loddo, R.; Tonelli, M.; Boido, V.; Laurini, E.; Posocco, P.; Fermeglia, M.; Pricl, S. *Bioorganic Med. Chem.* **2010**, 18 (16), 6055, https://doi.org/10.1016/j.bmc.2010.06.065.
4. Bari, A.; Grenier, D.; Azelmat, J.; Syed, S. A.; Al-Obaid, A. M.; Hosten, E. C. *Chem. Biol. Drug Des.* 94 **2019**, 4, 1750, https://doi.org/10.1111/cbdd.13576.
5. Tonelli, M.; Boido, V.; Canu, C.; Sparatore, A.; Sparatore, F.; Paneni, M. S.; Fermeglia, M.; Pricl, S.; La Colla, P.; Casula, L.; Ibba, C.; Collu, D.; Loddo, R. *Bioorganic Med. Chem.* **2008**, 16 (18), 8447, https://doi.org/10.1016/j.bmc.2008.08.028.
6. Saha, S. J.; Siddiqui, A. A.; Pramanik, S.; Saha, D.; De, R.; Mazumder, S.; Debsharma, S.; Nag, S.; Banerjee, C.; Bandyopadhyay, U. *ACS Infect. Dis.* **2019**, 5 (1), 63, https://doi.org/10.1021/acsinfecdis.8b00178.
7. Su, X.; Aprahamian, I. *Chemical Society Reviews.* **2014**, March 21, 1963, https://doi.org/10.1039/c3cs60385g.
8. Burdette, S. C. *Nat. Chem.* **2012**, 4 (9), 695, https://doi.org/10.1038/nchem.

9. Feringa, B. L.; Browne, W. R. *Molecular Switches* **2011**, Vol. I, II; Feringa, B. L., Browne, W. R., Eds.; Wiley-VCH Verlag GmbH & Co. KGaA: Weinheim, https://doi.org/10.1002/9783527634408.
10. Xu, W.; Shao, Z.; Han, Y.; Wang, W.; Song, Y.; Hou, H. **2018**, Elsevier Ltd., 152, 171, https://doi.org/10.1016/j.dyepig.2018.01.056.
11. Lukeš, V.; Michalík, M.; Poliak, P.; Cagardová, D.; Végh, D.; Bortňák, D.; Fronc, M.; Kožíšek, J. *Terminal Unit. Synth. Met.* **2016**, 219, 83, https://doi.org/10.1016/j.synthmet.2016.05.010.
12. Sandoval-Torrientes, R.; Pascual, J.; García-Benito, I.; Collavini, S.; Kosta, I.; Tena-Zaera, R.; Martín, N.; Delgado, J. L. *ChemSusChem.* **2017**, 10 (9), 2023, https://doi.org/10.1002/cssc.201700180.
13. Beverina, L.; Drees, M.; Facchetti, A.; Salamone, M.; Ruffo, R.; Pagani, G. A. *European J. Org. Chem.* **2011**, 28, 5555, https://doi.org/10.1002/ejoc.201100940.
14. Patrascu, B.; Lete, C.; Popescu, C.; Matache, M.; Paun, A.; Madalan, A.; Ionita, P. Arkivoc **2020**, vi, 1
15. Asadi, S.; Alizadeh-Bami, F.; Mehrabi, H. Arkivoc **2020**, vi, 0
16. Fateh V. Singha, F. V.; Wirth, T. Arkivoc **2021**, vii, 0
17. Eloh, K.; Demurtas, M.; Deplano, A.; Mfopa, A. N.; Murgia, A.; Maxia, A.; Onnis, V.; Caboni, P. *J. Agric. Food Chem.* **2015**, 63 (45), 9970, https://doi.org/10.1021/acs.jafc.5b04815.
18. Ghosh, P.; Hazra, A.; Ghosh, M.; Chandra Murmu, N.; Banerjee, P. *J. Mol. Struct.* **2018**, 1157, 444, https://doi.org/10.1016/j.molstruc.2017.12.007.
19. Chowdhury, A. R.; Ghosh, P.; Roy, B. G.; Mukhopadhyay, S. K.; Murmu, N. C.; Banerjee, P. *Aqueous Solvent. Sensors Actuators B. Chem.* **2015**, 220, 347, https://doi.org/10.1016/j.snb.2015.05.044.
20. Frisch, M. J.; Trucks, G. W.; Schlegel, H. B.; Scuseria, G. E.; Robb, M. A.; Cheeseman, J. R.; Scalmani, G.; Barone, V.; Petersson, G. A.; Nakatsuji, H.; Li, X.; Caricato, M.; Marenich, A. V.; Bloino, J.; Janesko, B. G.; Gomperts, R.; Mennucci, B.; Hratchian, H. P.; Ortiz, J. V.; Izmaylov, A. F.; Sonnenberg, J. L.; Williams-Young, D.; Ding, F.; Lipparini, F.; Egidi, F.; Goings, J.; Peng, B.; Petrone, A.; Henderson, T.; Ranasinghe, D.; Zakrzewski, V. G.; Gao, J.; Rega, N.; Zheng, G.; Liang, W.; Hada, M.; Ehara, M.; Toyota, K.; Fukuda, R.; Hasegawa, J.; Ishida, M.; Nakajima, T.; Honda, Y.; Kitao, O.; Nakai, H.; Vreven, T.; Throssell, K.; Montgomery, J. A. Jr.; Peralta, J. E.; Ogliaro, F.; Bearpark, M. J.; Heyd, J. J.; Brothers, E. N.; Kudin, K. N.; Staroverov, V. N.; Keith, T. A.; Kobayashi, R.; Normand, J.; Raghavachari, K.; Rendell, A. P.; Burant, J. C.; Iyengar, S. S.; Tomasi, J.; Cossi, M.; Millam, J. M.; Klene, M.; Adamo, C.; Cammi, R.; Ochterski, J. W.; Martin, R. L.; Morokuma, K.; Farkas, O.; Foresman, J. B.; Fox, D. J. *Gaussian* 16, Revision D.01 **2016**, Gaussian, Inc., Wallingford CT.
21. Spackman, M. A.; McKinnon, J. J.; Jayatilaka, D. *CrystEngComm.* **2008**, 10, 377.
22. Spackman, M. A.; Jayatilaka, D. *CrystEngComm* **2009**, 11, 19, *Chemistry* M313 **2008**, School of Biomedical, Biomolecular and Chemical Sciences, University of Western Australia, doi: 10.1039/B818330A.
23. Jayatilaka, D.; Grimwood, D. J.; Lee, A.; Lemay, A.; Russel, A. J.; Taylor, C.; Wolff, S. K.; Cassam-Chenai, P.; Whitton, A. **2005**, TONTO, http://hirshfeldsurface.net/.
24. Sheldrick, G. M. SHELXS *Acta Cryst.* A64 **2008**, 112.
25. Burla, M. C.; Caliandro, R.; Carrozzini, B.; Cascarano, G. L.; Cuocci, C.; Giacovazzo, C.; Mallamo, M.; Mazzone, A.; Polidori, G. *J. Appl. Cryst.* 48 **2015**, 306, https://doi.org/10.1107/S1600576715001132.
26. Sheldrick, G. M. SHELXL *Acta Cryst.* C71 **2015**, 3, https://doi.org/10.1107/S2053229614024218.
27. Brandenburg, K. Crystal Impact GbR Bonn, Germany **1999**.
28. Turner, M. J.; McKinnon, J. J.; Wolff, S. K.; Grimwood, D. J.; Spackman, P. R.; Jayatilaka, D.; Spackman, M. A. *CrystalExplorer 17.5* **2017**, University of Western Australia.

29. Dolomanov, O. V.; Bourhis, L. J.; Gildea, R. J.; Howard, J. A. K.; Puschmann, H. *J. Appl. Cryst.* 42 **2009**, 339, https://doi.org/10.1107/S0021889808042726.
30. Spek, A. L. *J. Appl. Cryst.* **2003**, 36, 7, https://doi.org/10.1107/S0021889802022112.
31. Hübschle, Ch. B.; Sheldrick, G. M.; Dittrich, B. *J. App. Cryst.* 44 **2011**, 1281, https://doi.org/10.1107/S0021889811043202.
32. Stoe & Cie *X-Area Recipe* 1.33.0.0. Stoe & Cie GmbH **2015**, Darmstadt, Germany.
33. Stoe & Cie *X-Area Pilatus3_SV* 1.31.150.0. Stoe & Cie GmbH **2015**, Darmstadt, Germany.
34. Stoe & Cie *X-AREA Integrate*. Stoe & Cie GmbH **2018**, Darmstadt, Germany.
35. Stoe & Cie *X-AREA, X-RED32 and X-SHAPE*. Stoe & Cie GmbH 2017, Darmstadt, Germany.
36. Allen, F. H.; Kennard, O.; Watson, D. G.; Brammer, L.; Orpen, A. G.; Taylor, R. *J. of the Chemical Society, Perkin Transactions 2* **1987**, 12, S19, http://dx.doi.org/10.1039/p298700000s1.
37. Collin, R. L.; Lipscomb,W. N. *Acta Cryst.* **1951**, 4, 10.
38. Wiberg, K. B. *Tetrahedron **1968***, 24, 3, 1083, https://doi.org/10.1016/0040-4020(68)88057-3.
39. Bernstein, J.; Davis, R. E.; Shimoni, L.; Chang, N. L. *Angew. Chem. Int Ed. Engl.* **1995**, 34, 1555, https://doi.org/10.1002/anie.199515551.
40. Hypercube, Inc. Hyperchem 7.0 **2007**, Gainesville, FL, 32601, USA.
41. CrysAlisPro Software system, Version 1.171.37.31. release 14-01-2014 CrysAlis171 .NET. Agilent Technologies UK Ltd., Oxford, UK.
42. Bortňák, D. ; Pecher, D. ; Végh, D. ; Breza, M. ; Mikuš, P. ; Milata, V. *J. of Mass Spectrometry* **2020**, 55(10), e4540, DOI: 10.1002/jms.4540